STEM CELLS TRANSLATIONAL MEDICINE®

TISSUE ENGINEERING AND REGENERATIVE MEDICINE

Remotely Activated Mechanotransduction via Magnetic Nanoparticles Promotes Mineralization Synergistically With Bone Morphogenetic Protein 2: Applications for Injectable Cell Therapy

JAMES R. HENSTOCK,[a] MICHAEL ROTHERHAM,[a] HASSAN RASHIDI,[b] KEVIN M. SHAKESHEFF,[b] ALICIA J. EL HAJ[a]

Key Words. Bone marrow stromal cells • Cellular therapy • Clinical translation • Differentiation • Mesenchymal stem cells • Tissue regeneration • Transduction

[a]Institute for Science and Technology in Medicine, Keele University, Stoke-on-Trent, United Kingdom; [b]School of Pharmacy, University of Nottingham, Nottingham, United Kingdom

Correspondence: James R. Henstock, Ph.D., Institute for Science and Technology in Medicine, Keele University, Guy Hilton Research Centre, Thornburrow Drive, Hartshill, Stoke-on-Trent ST4 7QB, United Kingdom. Telephone: 44-7793-886098; E-Mail: j.r.henstock@keele.ac.uk

Received January 28, 2014; accepted for publication July 7, 2014; first published online in SCTM *Express* September 22, 2014.

1066-5099/2014/$20.00/0

http://dx.doi.org/10.5966/sctm.2014-0017

ABSTRACT

Bone requires dynamic mechanical stimulation to form and maintain functional tissue, yet mechanical stimuli are often lacking in many therapeutic approaches for bone regeneration. Magnetic nanoparticles provide a method for delivering these stimuli by directly targeting cell-surface mechanosensors and transducing forces from an external magnetic field, resulting in remotely controllable mechanotransduction. In this investigation, functionalized magnetic nanoparticles were attached to either the mechanically gated TREK1 K^+ channel or the (integrin) RGD-binding domains of human mesenchymal stem cells. These cells were microinjected into an ex vivo chick fetal femur (embryonic day 11) that was cultured organotypically in vitro as a model for endochondral bone formation. An oscillating 25-mT magnetic field delivering a force of 4 pN per nanoparticle directly against the mechanoreceptor induced mechanotransduction in the injected mesenchymal stem cells. It was found that cells that received mechanical stimuli via the nanoparticles mineralized the epiphyseal injection site more extensively than unlabeled control cells. The nanoparticle-tagged cells were also seeded into collagen hydrogels to evaluate osteogenesis in tissue-engineered constructs: in this case, inducing mechanotransduction by targeting TREK1 resulted in a 2.4-fold increase in mineralization and significant increases in matrix density. In both models, the combination of mechanical stimulation and sustained release of bone morphogenetic protein 2 (BMP2) from polymer microspheres showed a significant additive effect on mineralization, increasing the effectiveness of BMP2 delivery and demonstrating that nanoparticle-mediated mechanotransduction can be used synergistically with pharmacological approaches for orthopedic tissue engineering to maximize bone formation. STEM CELLS TRANSLATIONAL MEDICINE *2014;3:1363–1374*

INTRODUCTION

Mechanotransduction is an important factor in bone metabolism and an essential component in postoperative orthopedic physiotherapy and rehabilitation. However, mechanotransduction is often neglected in severe cases of nonunion because of the difficulties in patient mobilization, whereas stress shielding is a known drawback of many materials used in orthopedic repair [1]. Substantial evidence suggests that mechanical stimuli play a role in the osteoblastic differentiation of mesenchymal stem cells, interacting with and amplifying signaling cascades from growth factors such as bone morphogenetic proteins (BMPs) [2, 3]. As a result, the presence or absence of mechanical stimulation during stem cell differentiation and tissue synthesis can have a large impact on the quality and quantity of bone formed, potentially affecting the clinical outcome of treatments for nonunion and the integration of articular prostheses.

Providing appropriate mechanical stimuli to injectable or implantable stem cells is therefore a major challenge for translational medicine. Although it may be difficult to directly apply mechanical loads to bone defects without causing further damage, various indirect methods have been used in attempts to stimulate mechanotransduction in situ. Low-intensity pulsed ultrasound has found some success in directing microstrain to healing bone, but data from clinical trials are conflicted in determining its effectiveness [4]. Similarly, piezoelectric biomaterials or oscillating electrical fields may propagate microstrain to repairing bone, but these treatments are still at an experimental stage [5, 6].

Previous research has demonstrated that cell-surface mechanoreceptors can be directly targeted using functionalized magnetic nanoparticles

and then excited using external magnetic fields [7]. Targeting specific receptors, such as the mechanically gated ion channel TREK1 [8–11] and the Arg-Gly-Asp (RGD)-binding sites of integrins that connect the intracellular cytoskeleton to the extracellular matrix [12], permits external control of pathway activation. Applying an external oscillating electromagnetic field to the magnetic nanoparticle creates a piconewton torque that is transferred to the protein, ion channel, or receptor to which it has attached, propagating the mechanical stimulus via mechanotransduction pathways inside the cell. Therefore, mechanotransduction is stimulated without causing mechanical stress to the construct or surrounding tissue and allowing a range of stimulation frequencies and forces to be applied through a choice of target receptors. A detailed analysis of this bioreactor technology is given by Hughes et al. [11].

In this investigation, we have tested the potential effectiveness of remotely activated mechanotransduction as a component of injectable cell-based therapies using two relevant models of bone formation: firstly, an organotypically cultured ex vivo developing chick fetal femur, and secondly, a tissue-engineered collagen hydrogel. The chick fetal femur is a useful model system for studying endochondral bone formation in vitro [13–15] because isolation of the femoral anlagen midway through gestation (day 11 or Hamburger and Hamilton stages 33–35) [16] provides a cartilaginous rudiment with a single mineralization site (the bone collar) and an absence of either epiphyseal mineralization or osteoclasts. The organotypic culture model therefore allows the progress of mineralization to be monitored in response to applied experimental treatments, and the osteogenic effects of nanoparticle-mediated mechanotransduction at injection sites can be accurately determined using x-ray microtomography [17]. Cell-seeded collagen hydrogels were also used to investigate the action of the targeted nanoparticles under more finely controlled conditions and to demonstrate how this methodology might augment biomaterial strategies for regenerative medicine.

We have also studied the interaction of nanoparticle-mediated mechanotransduction with sustained release of the growth factor BMP2, delivered via bioresorbable polymer microparticles as an example of a combination strategy for tissue engineering. These microparticles have controllable release kinetics and have generated successful results both in vitro and in preclinical models [18–20]. The ability to provide sustained or staged release of pharmaceuticals from these microparticles when injected into wound sites allows for growth factor delivery to be controlled both spatially and temporally [20].

The aims of this work were to evaluate the osteogenic differentiation of human stem cells and subsequent bone formation in appropriate three-dimensional culture models in response to the remote activation of mechanotransduction pathways both as a primary osteogenic stimulus and in combination with the sustained delivery of BMP2.

Materials and Methods

Chick Fetal Femur Culture

Intact femurs were removed from freshly killed Dekalb white chick fetuses after 11 days of gestation and carefully cleaned of all muscle tissue by rolling on sterile tissue. Femurs measured approximately 7 mm at isolation and were organotypically cultured ex vivo on porous polycarbonate membrane inserts in 6-well cell culture plates as described by Kanczler et al. [14] and Smith et al. [15] in 1-ml osteogenic α-modified Eagle's medium containing 1% penicillin-streptomycin and 150 $\mu g \cdot ml^{-1}$ ascorbic acid, 2 mM sodium β-glycerophosphate, and 10^{-8} M dexamethasone (all from Sigma-Genosys, Cambridge, U.K., http://www.sigmaaldrich.com/Brands/Sigma_Genosys.html). The femurs were cultured for 14 days in total at 37°C and at 5% CO_2 in a humidified incubator, with culture medium being completely replaced every 24 hours.

Human Mesenchymal Stem Cell Culture

Human mesenchymal stem cells were obtained from a bone marrow aspirate (Lonza) and cultured to p3 in basal Dulbecco's modified Eagle's medium (DMEM) containing 10% fetal calf serum and 1% penicillin-streptomycin.

Magnetic Nanoparticle Labeling

One milligram of Nanomag superparamagnetic nanoparticles (carboxyl-coated, 300 nm in diameter; Micromod, Rostock, Germany, http://www.micromod.de) were surface-activated by washing in sterile 1-ethyl-3-(3-dimethylaminopropyl)-carbodiimide hydrochloride and *N*-hydroxysuccinimide in 0.5 M MES buffer, adjusted to pH 6.3 with Na_2CO_3 for 1 hour at room temperature, recovered by magnetic separation, and washed in 0.1 M MES buffer. One milligram of nanoparticles were then conjugated to either 10 μg of RGD-tripeptide or 10 μg of TREK1-Ab (Alomone Labs, Jerusalem, Israel, http://www.alomone.com) by mixing together in 1 ml of 0.1 M MES buffer for 3 hours. Attachment of the RGD-coated nanoparticles to their targets in the mesenchymal stem cells (MSCs) was achieved by culturing the human MSCs (hMSCs) in suspension in serum-free media for 3 hours followed by incubation with 125 μg of particles per 10^6 cells with intermittent agitation. The cells were centrifuged, washed, and immediately used in experiments. Because the TREK1 antibody epitope is intracellular, these particles were first coated in 40 ng of *N*-[1-(2,3-dioleoyloxy)propyl]-*N*,*N*,*N*-trimethylammonium methyl-sulfate to aid nanoparticle uptake.

BMP2 Microparticle Encapsulation

Poly(vinyl alcohol) (PVA; molecular weight, 13,000–23,000 Da, 87%–89% hydrolyzed), human serum albumin (HSA), poly(D,L-lactide-coglycolide) (PLGA) polymers with lactide: glycolide ratios of 50:50 (DLG 4.5A 59 kDa) were purchased from SurModics (Birmingham, AL, http://www.surmodics.com). Recombinant human BMP2 was purchased from Prof. Walter Sebald (University of Wurzburg, Wurzburg, Germany). Poly(D,L-lactide-coglycolide) microparticles were formed using a water-in-oil-in-water emulsion method as previously described [13]. Briefly, triblock copolymer was added to PLGA to provide weight percentages of 30% (wt/wt) of the 1 g of total mass in 5 ml of dichloromethane. BMP2 and HSA solution were prepared at a ratio of 1:9 for a 1% (wt/wt) loading in the microparticles. In order to manufacture microparticles, the aqueous solution of HSA and BMP2 was added to a solution of PLGA-tri block copolymer. These phases were homogenized for 2 minutes at 4,000 rpm in a Silverson L5M homogenizer (Silverson Machines, Chesham, U.K., http://www.silverson.com) to form the water-in-oil emulsion. This primary emulsion was transferred to 200 ml of 0.3% (wt/vol) PVA solution and was homogenized for a second time at 9,000 rpm. The resultant double emulsion was stirred at 300 rpm on a Variomag 15-way magnetic stirrer for a minimum of 4 hours to facilitate dichloromethane evaporation. Microparticles were then washed

and lyophilized (Edwards Modulyo; IMA Edwards, Alcester, U.K., http://www.ima-pharma.com) until dry. The particle size range was 10–40 μm in diameter. The sustained release formulation was engineered to give 30% burst release on day 1 followed by 5% daily release. The loading was 0.4 mg of BMP2 in 1 g of polymer with 50% entrapment efficiency. Using 1-mg particles per individual hydrogel or injection, the release kinetics were therefore 60 ng per day followed by 10 ng per day.

Microinjection

MSCs prelabeled with nanoparticles were introduced into three sites in the femur (both cartilaginous epiphyses and the midpoint of the diaphyseal bone collar) using a 1-ml syringe microinjection system (Linton Instrumentation, Diss, U.K., http://www.lintoninst.co.uk) and a glass capillary needle with a ~70-μm tip diameter. Then 10^3 cells were injected in a volume of 20 nl. Microinjections were performed under sterile conditions with the aid of a dissecting microscope. Coinjections containing BMP2 microspheres used a suspension containing both cells and microspheres.

Collagen Hydrogels

Human MSCs were seeded into 2 mg/ml collagen hydrogels made from a stock solution of 9.21 mg/ml rat tail collagen (type I). Hydrogel pellets each containing 10^4 cells were made by dispensing 300 μl of this hydrogel into permeable Transwell inserts (Corning Enterprises, Corning, NY, http://www.corning.com) in a 24-well plate and neutralized using culture media. Contraction of the hydrogels caused by cell attachment was allowed to occur to generate scaffolds in which cells were relatively unstressed, and a reduction in volume to approximately 3 mm^3 occurred within 72 hours. Cells were labeled with the nanoparticles prior to the original seeding into the hydrogel, and the constructs were cultured for 28 days in osteogenic DMEM containing dexamethasone, sodium β-glycerophosphate, and asborbic acid.

Magnetic Force Bioreactor

Magnetically stimulated groups were placed in an incubator (37°C, 5% CO_2) above a custom-built vertical oscillating magnetic force bioreactor (MICA Biosystems, Stoke-on-Trent, U.K., http://micabiosystems.com), thus maintaining otherwise standard culture conditions. Nonstimulated control groups were kept in identical conditions (without magnetic field). Magnetically stimulated groups were exposed to a maximum 25-mT magnetic field from an array of permanent magnets (NdFeB) situated beneath the culture plates at a frequency of 1 Hz (Fig. 1). Magnetic stimulation was performed in daily 1-hour sessions for 14 days (microinjected femurs) or 28 days (hMSC-seeded hydrogels).

X-Ray Microtomography

Endpoint analysis of the femurs and hydrogels was primarily by x-ray microtomography (μCT) using a Scanco (Brüttisellen, Switzerland, http://www.scanco.ch) μCT40 (beam energy, 55 kVp; beam intensity, 145 μA; integration time, 200 ms; spatial resolution, 10 μm). Femurs were analyzed at two density thresholds (50/1,000 and 120/1,000), firstly at a lower threshold to determine the total size, volume, and average density of each femur following treatment and secondly at a higher threshold to quantify the extent of osteogenesis in the femur and the mineralized bone density. The thresholds were conserved throughout these experiments, allowing for direct comparison of bone formation across the investigation. The hydrogels were also analyzed at two density thresholds (50/1,000 and 80/1,000) to determine the amount of mineralizing matrix within the construct. All analysis on the reconstructions was performed using Scanco software tools.

Histological Staining

Femurs and hydrogels were fixed in 4% paraformaldehyde for 48 hours and washed in phosphate-buffered saline (PBS). Whole-mount histological staining for calcium deposition was performed by immersing the femurs and hydrogels in 1% alizarin red solution for 1 hour followed by washing in PBS and imaging using a dissecting microscope fitted with a Nikon (Tokyo, Japan, http://www.nikon.com) D500 digital camera. Visualization of collagen condensation in the hydrogels was performed by fixing the samples as above and staining the constructs with a 1% solution of Sirius red in water, followed by three washes in 1× PBS. Microscopic analysis of tissue sections was achieved by embedding the femurs in optimal cutting temperature compound and cutting 10-μm sections using a microtome-cryostat. Sections were stained with aqueous 1% alizarin red solution for calcium and Alcian blue (in 0.1 M hydrochloric acid) for glycosaminoglycans (both from Sigma-Genosys).

Calcium Quantification

Quantification of calcium in the hydrogels was by immersing the alizarin-stained samples in 5% cetylpyridinium chloride (Sigma-Genosys) solution for 24 hours, yielding a purple destain solution containing the cetylpyridinium-alizarin complex, which was quantified at 562 nm. Following the destain, some calcium deposits strongly associated with the matrix remained stained.

Alkaline Phosphatase Activity

Alkaline phosphatase activity in the culture medium was measured by taking a 50-μl sample of the medium and quantifying the dephosphorylation of *p*-nitrophenyl phosphate, a phosphatase substrate that turns yellow (λ_{max}= 405 nm) when dephosphorylated by alkaline phosphatase after 10 minutes of incubation at room temperature.

RESULTS

MSCs were microinjected into the femur by inserting the tip of a glass capillary needle into the cartilaginous rudiment and withdrawing to create a small cavity without excessively damaging the surrounding tissue. 20 nl of PBS containing the cell suspension was delivered via a micrometer-driven syringe, and the femurs were returned to organotypic culture on Transwell membranes. Membrane labeling the MSCs with DiO allowed the microinjection to be confirmed (Fig. 2A, 2B). After 14 days of in vitro culture, femur epiphyses from sham control groups (Fig. 2C, 2D) and femurs injected with TREK1 magnetic nanoparticle-labeled hMSCs (Fig. 2E, 2F) were histologically stained for glycosaminoglycans (blue) and calcium (red). Damage to the cell layers at the injection site appeared to stimulate mineralization by periosteal cells in the sham-injected control groups, whereas epiphyses injected with TREK1-labeled MSCs showed more widespread mineralization in the entire region surrounding the injection site.

Visual examination of x-ray microtomography reconstructions of the femurs (Fig. 3A–3H) revealed in detail that the

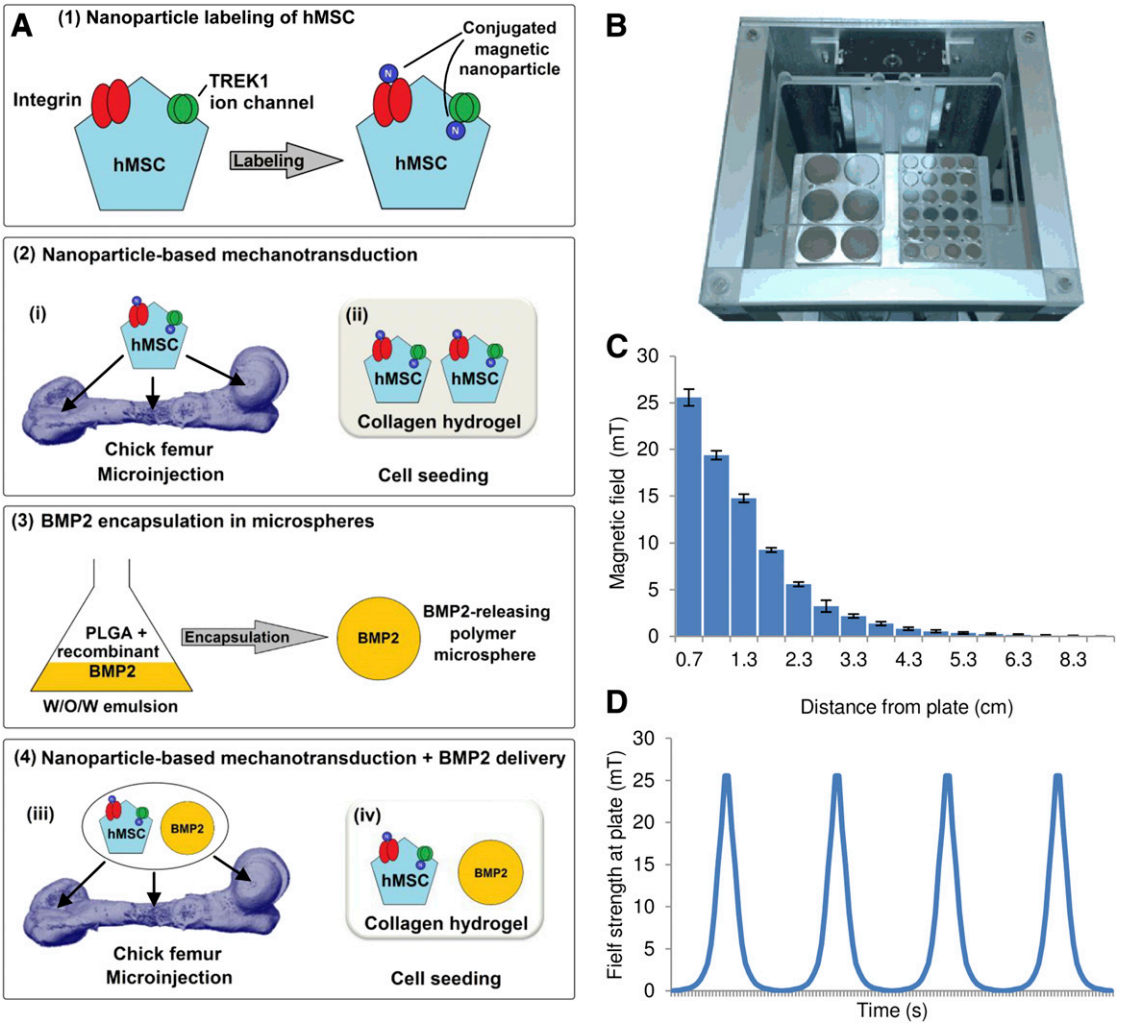

Figure 1. Experimental overview. **(A):** Schematic of the experimental design. **(A1):** hMSCs were labeled with magnetic nanoparticles targeting either the Arg-Gly-Asp-binding domains of cell-surface molecules such as integrins or the TREK1 mechanosensitive ion channel. **(A2):** The cells were then either injected into a cultured ex vivo chick femur **(A2i)** or seeded into a collagen hydrogel scaffold **(A2ii)**. **(A3):** In subsequent experiments, the combined effects of directed mechanotransduction and BMP2 delivery were studied using BMP2-releasing poly(D,L-lactide-cogly-colide) microspheres formed by an emulsion method. **(A4):** Labeled cells and BMP2-releasing microspheres were codelivered into either the chick femur or collagen hydrogels. **(B):** The nanoparticle-receptor complex was stimulated using a vertically oscillating external field delivered by a moving magnetic array situated beneath the culture plates for 1 hour per day (Mica Biosystems bioreactor). **(C):** The maximum magnetic field strength experienced at the plate was ~25 mT, which attenuated rapidly as the array was withdrawn. **(D):** The cycle was repeated at 1 Hz. Abbreviations: BMP2, bone morphogenetic protein 2; hMSC, human mesenchymal stem cells; W/O/W, water-in-oil-in-water emulsion.

epiphyses were becoming mineralized at and surrounding the sites of microinjection. Epiphyseal mineralization was observed in some sham-injected femurs, but mineralization was more prevalent and significantly greater in extent in the femurs injected with nanoparticle-labeled cells. The diaphyseal injection site was not apparent after 2 weeks of culture, although irregular areas in the injected region were visible in some femurs.

Femurs injected with unlabeled hMSCs (no nanoparticles) showed similar alkaline phosphatase activity and mineralization to controls, which were sham-injected with PBS. Similarly, the oscillating magnet alone had no effect (Fig. 3I). Injecting hMSCs labeled with either RGD-coated or anti-TREK1 magnetic nanoparticles resulted in both increased alkaline phosphatase activity and mineralization in the femur. Microinjection of hMSCs labeled with RGD-coated magnetic nanoparticles resulted in an average 34% increase in the extent of mineralization, whereas injecting cells labeled with TREK-Ab-coated magnetic nanoparticles caused an average 31% increase in the volume of the bone formed (Fig. 3J).

Seeding nanoparticle-labeled MSCs into collagen hydrogels allowed greater control over the initial cell-seeding conditions and permitted the bone formation process to be observed in more detail (Fig. 4A). After 28 days of in vitro culture, analysis by μCT revealed that the volume of higher density condensed mineralizing matrix in the cell-seeded hydrogels was similar for all controls and that the oscillating magnetic field had no effect on unlabeled cells (without nanoparticles). Adding RGD-conjugated magnetic nanoparticles directly to the gel (without prelabeling the cells) did not result in any increase in volume or density of the gel compared with controls, demonstrating that specific binding of the nanoparticles to the target cellular epitope was required to achieve mechanotransduction. Prelabeling the

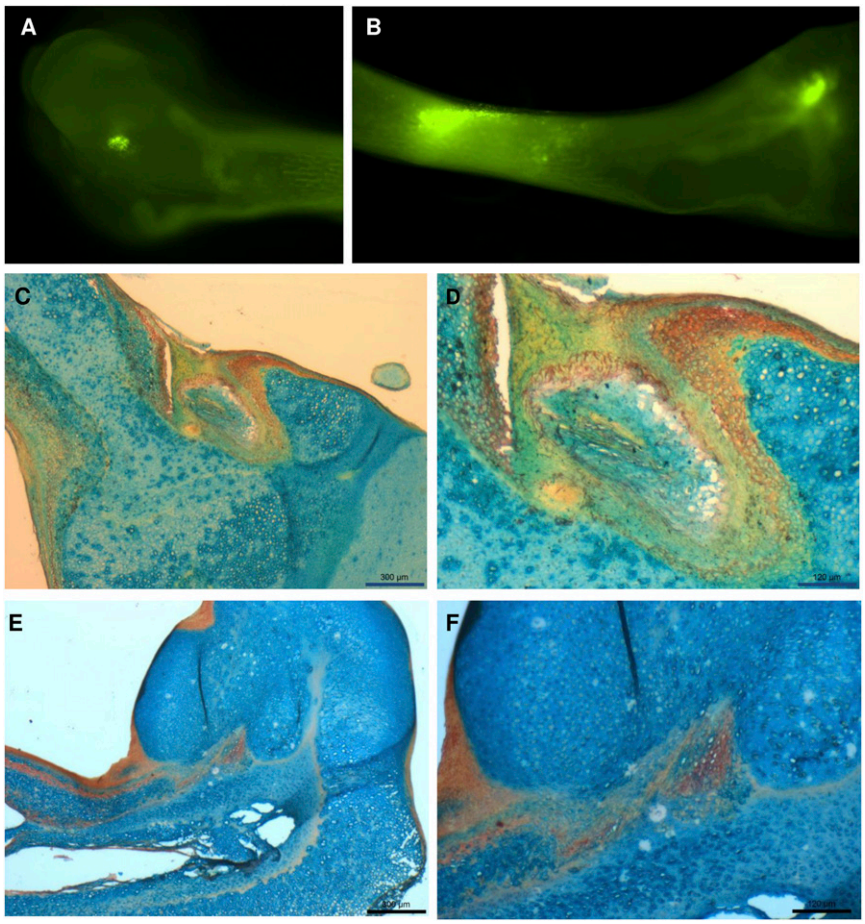

Figure 2. Microinjection into the chick fetal femur. **(A, B):** Human mesenchymal stem cells (hMSCs) labeled with the live cell tracker membrane dye DiL and injected into both cartilaginous epiphyses **(A)** and the middiaphysis **(B)**, imaged immediately after microinjection. **(C–F):** After 2 weeks of ex vivo organotypic culture, femur epiphyses from sham control groups **(C, D)** and femurs injected with TREK1 magnetic nanoparticle-labeled hMSCs **(E, F)** were sectioned and histologically stained for glycosaminoglycans (blue) and calcium (red). Damage to the cell layers at the injection site appears to stimulate mineralization in the sham-injected control groups, whereas the nanoparticle-injected epiphyses show more widespread mineralization distal to the injection site. Scale bars = 300 μm **(C, E)** and 120 μm **(D, F)**.

cells with RGD-coated nanoparticles before seeding into the gel resulted in significant increases in both volume (1.86-fold increase, $p = 6.9 \times 10^{-7}$) and density (1.13-fold increase, $p = 3 \times 10^{-4}$). Cells labeled with anti-TREK1 nanoparticles showed the greatest increases in volume (2.44-fold increase, $p = 2 \times 10^{-4}$) and density (1.28-fold increase, $p = 6 \times 10^{-11}$).

Visual analysis of the cell-seeded hydrogels by μCT reconstructions (Fig. 4B) and whole-mount staining for collagen (Fig. 4C) or calcium (Fig. 4D) revealed that all control groups showed similarly amorphous patterns of matrix condensation and mineralization with no localized concentrations of either collagen or calcium within the gel. However, hydrogels containing hMSCs prelabeled with either RGD- or TREK1-nanoparticles contained large areas of mineralization that were visible as extensive condensed regions on μCT reconstructions and stained intensely for both collagen and calcium (Fig. 4B–4D). Quantification of the calcium deposition using a destaining solution confirmed that both nanoparticle-labeled groups were significantly more mineralized than controls (Fig. 4E).

In the second set of experiments, PLGA microspheres that release BMP2 were coinjected with hMSCs labeled with either RGD- or TREK-Ab-coated nanoparticles. The sustained release formulation was engineered to deliver BMP2 as a 60-ng burst release on day 1 followed by 10 ng daily release. Microinjection in this case was more challenging because of the accumulation of the microspheres in the needle tip. Staining the femurs with alizarin red for calcium deposition revealed the extent of the mineralization at the epiphyseal injection sites and also showed that the epiphyseal mineralization was frequently continuous with (or an extension of) the mineralizing bone collar (Fig. 5A–5G). BMP2 microspheres alone caused a nonsignificant increase in the volume of bone formed in this experiment, whereas injections of hMSCs labeled with either nanoparticle caused an increase in bone density (significant for RGD, $p = .013$; Fig. 5H). Combination injections of BMP2- and TREK-Ab-labeled cells resulted in significant increases in the density of the bone collar ($p = .048$).

The conditions for the above experiment were again replicated in a hMSC-seeded 2.0% collagen hydrogel to investigate the osteogenic combination of nanoparticle-labeled cells with BMP2-releasing microspheres (Fig. 6). Similar trends were observed to the chick femur injection study, because BMP2 alone caused a small increase in the volume of the construct, whereas either magnetic nanoparticle alone caused an increase in the density of the extracellular matrix. Combinations of BMP2

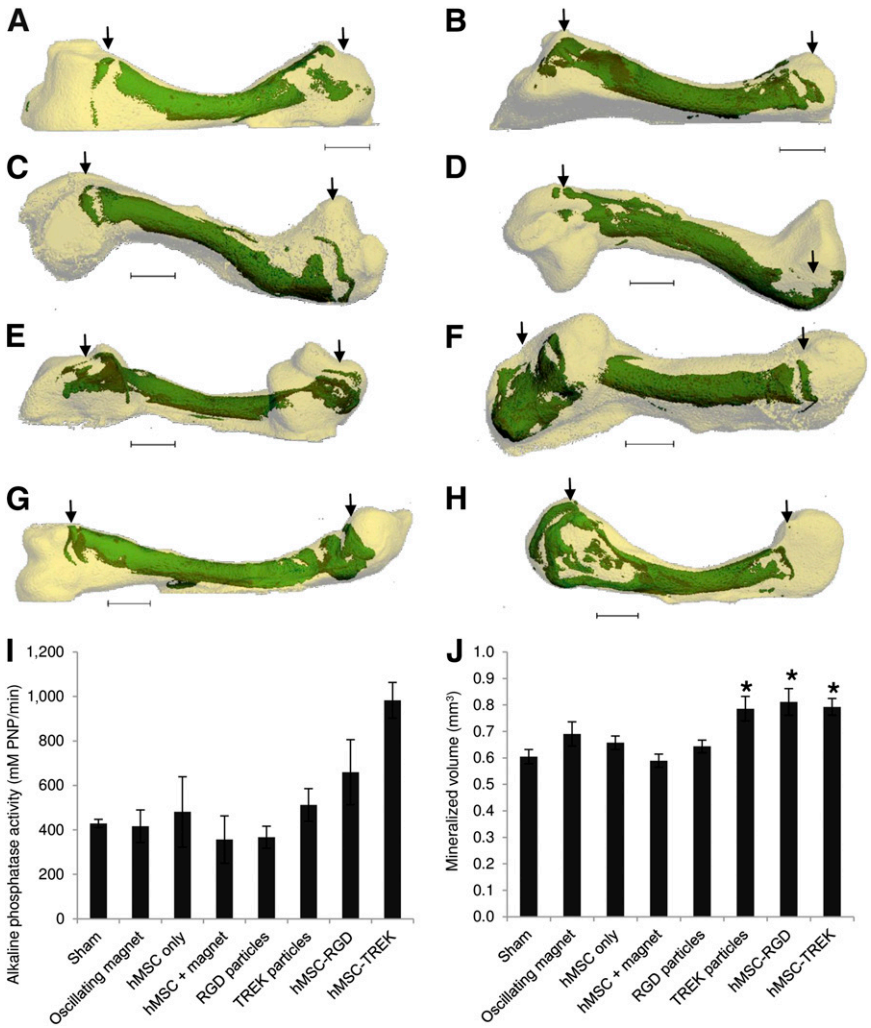

Figure 3. Mineralization in the chick fetal femur at the sites of microinjection. **(A–D):** Bone collars and secondary mineralization sites (green) within the cartilaginous chick fetal femur (white) showing the location and extent of mineralization following sham injection **(A)**, exposure to magnetic bioreactor alone **(B)**, injection of hMSCs **(C)**, and injection of hMSCs followed by exposure to the magnetic bioreactor **(D)**. **(E, F):** The addition of magnetic nanoparticles coated with RGD tripeptide **(E)** or TREK-Ab **(F)** resulted in mineralization at the epiphyseal injection sites. **(G, H):** Femurs injected with hMSCs prelabeled with either RGD-coated **(G)** or TREK-Ab-coated **(H)** magnetic nanoparticles showed the greatest extent of mineralization. Most femurs (including sham-injected femurs) displayed a secondary mineralization site in the epiphysis at the site of injection, whereas the diaphyseal injection site was not visible in any femur after 2 weeks of organotypic ex vivo culture. **(I, J):** After 14 days of in vitro culture, femurs injected with either phosphate-buffered saline (sham) or exposed to the oscillating magnetic bioreactor alone showed similar alkaline phosphatase activity **(I)** and mineralization **(J)** to injections of hMSCs and injections of RGD-coated magnetic nanoparticles alone. Injecting TREK-Ab-coated magnetic nanoparticles or hMSCs pretagged with either RGD or TREK nanoparticles caused significant increases in the extent of mineralization in the femur **(J)**, and tagged cells exhibited more alkaline phosphatase activity **(I)**. Arrows show the locations of the epiphyseal injections. Bars show standard error of the mean ($n = 3$ for alkaline phosphatase; $n = 9$ for x-ray microtomography). $*$, $p < .05$. Scale bars = 1 mm. Abbreviations: hMSC, human mesenchymal stem cells; PNP, *p*-nitrophenyl phosphate; RGD, Arg-Gly-Asp tripeptide.

microspheres and either nanoparticle resulted in significant increases in both volume and density ($p < .01$). BMP2 alone did not elicit increases in either volume or density at the higher mineralization threshold, but when used in combination with RGD-nanoparticles resulted in a fourfold increase in mineralized volume ($p = .063$). TREK-MNPs alone significantly increased the mineralized volume of the hydrogel from 0.013 to 0.051 mm^3, an increase of 3.8-fold, and the BMP2 plus TREK combination resulted in 0.084 mm^3 bone formation, 6.3-fold greater than controls ($p = 2 \times 10^{-5}$).

By treating the mineralized regions within the hydrogels as trabecular-like structures, a computed tomography analysis revealed that the nanoparticle + BMP combinations had thicker and more numerous mineralized regions within the hydrogel, although interestingly they were more isolated (significantly less interconnected) in the TREK-labeled groups, with or without BMP, compared with controls (Fig. 6C, 6D), which is observable in cross-section (Fig. 6E, 6F).

Discussion

Like many tissues, bone uses mechanical cues during its development and repair, combining both biochemical and strain gradients to form a tissue that has optimum strength in an appropriate orientation [21, 22]. The nature of mechanosensing in bone is complex, and a variety of force transduction

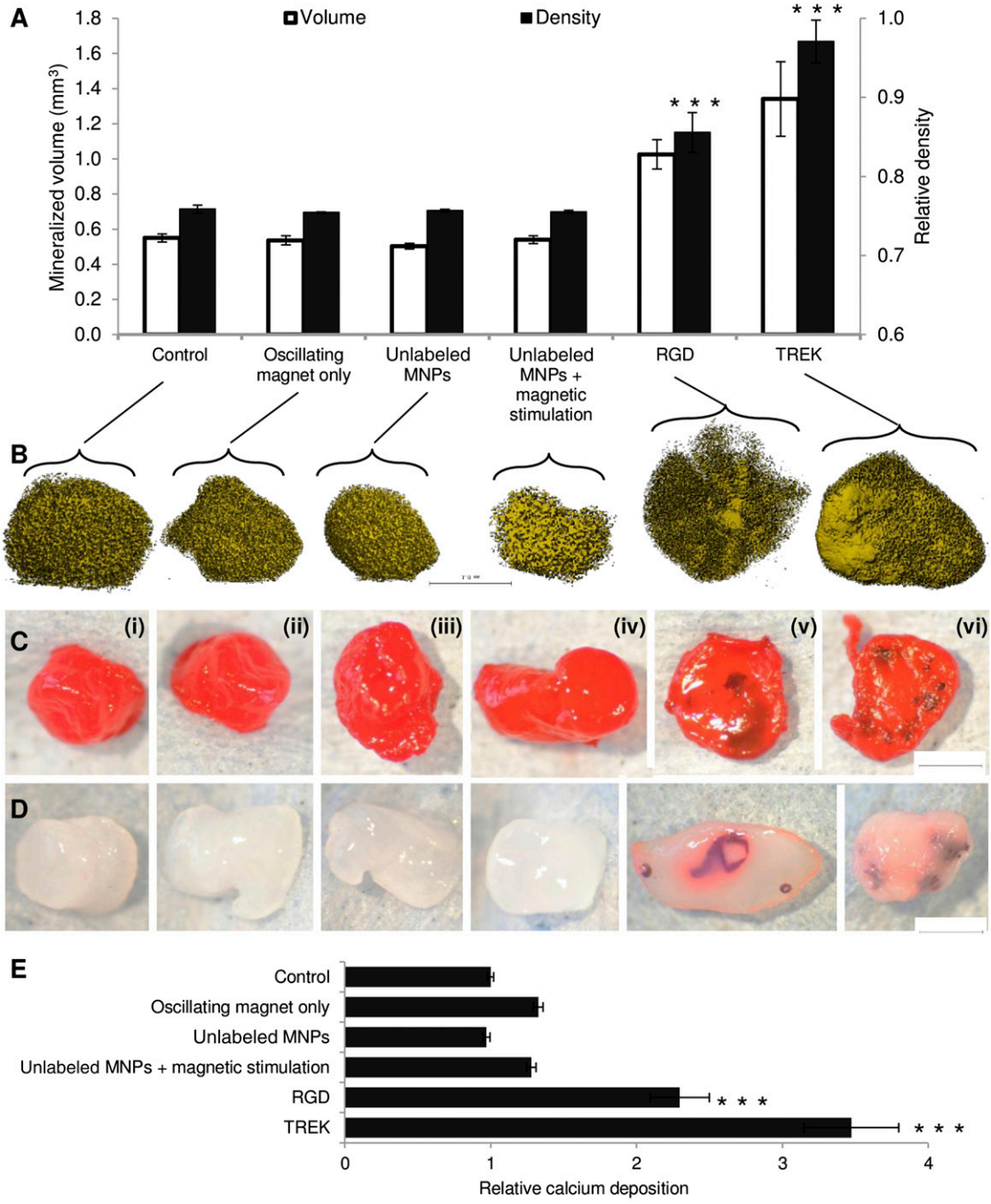

Figure 4. Effect of magnetic nanoparticles on human mesenchymal stem cells (hMSCs) cultured in vitro in collagen hydrogels. Controls included MSCs alone **(Ci)**, MSCs cultured with the oscillating field but no nanoparticles **(Cii)**, and RGD-conjugated nanoparticles in the hydrogel (but not attached to cells) both alone **(Ciii)** and with the oscillating magnetic field **(Civ)**. The experimental conditions included hydrogels seeded with MSCs prelabeled with RGD-coated nanoparticles **(Cv)** and TREK antibody-coated nanoparticles **(Cvi)**. **(A):** X-ray microtomography revealed that mineralization in the gels similar under all the control conditions. Both RGD- and TREK-Ab-conjugated magnetic nanoparticles had significant effects on both the volume and density of the mineralized material in the gel when the hMSCs were labeled prior to seeding into the hydrogel. **(B):** X-ray microtomography reconstructions showing the mineralizing higher density material within the seeded collagen hydrogels. **(C):** Sirius red staining for collagen. **(D):** Alizarin red staining for calcium following partial destaining with 1% cetylpyridinium chloride. All controls containing no MNPs or MNPs unattached to cells showed similarly amorphous and nonlocalized mineralization (microtomography [μCT]) with no concentrations of collagen or calcification remaining after partial destaining. Hydrogels containing cells prelabeled with either RGD- or TREK-Ab-conjugated magnetic nanoparticles formed large regions of high-density material (μCT), which stained intensely for collagen, showing up against the background 2% collagen hydrogel. Calcium deposition was similarly localized into nodules and ridges and was sufficiently bound to dense matrix as to resist being destained by 1% cetylpyridinium chloride solution. **(E):** Destaining allowed quantification of calcium deposition, which was equivalent for all controls and significantly greater in hydrogels seeded with RGD- and TREK-Ab-tagged cells. Scale bars = 1 mm. Error bars in **(A)** and **(E)** show standard error of the mean (n = 9). ***, $p < .001$. Abbreviations: MNPs, magnetic nanoparticles; RGD, Arg-Gly-Asp tripeptide.

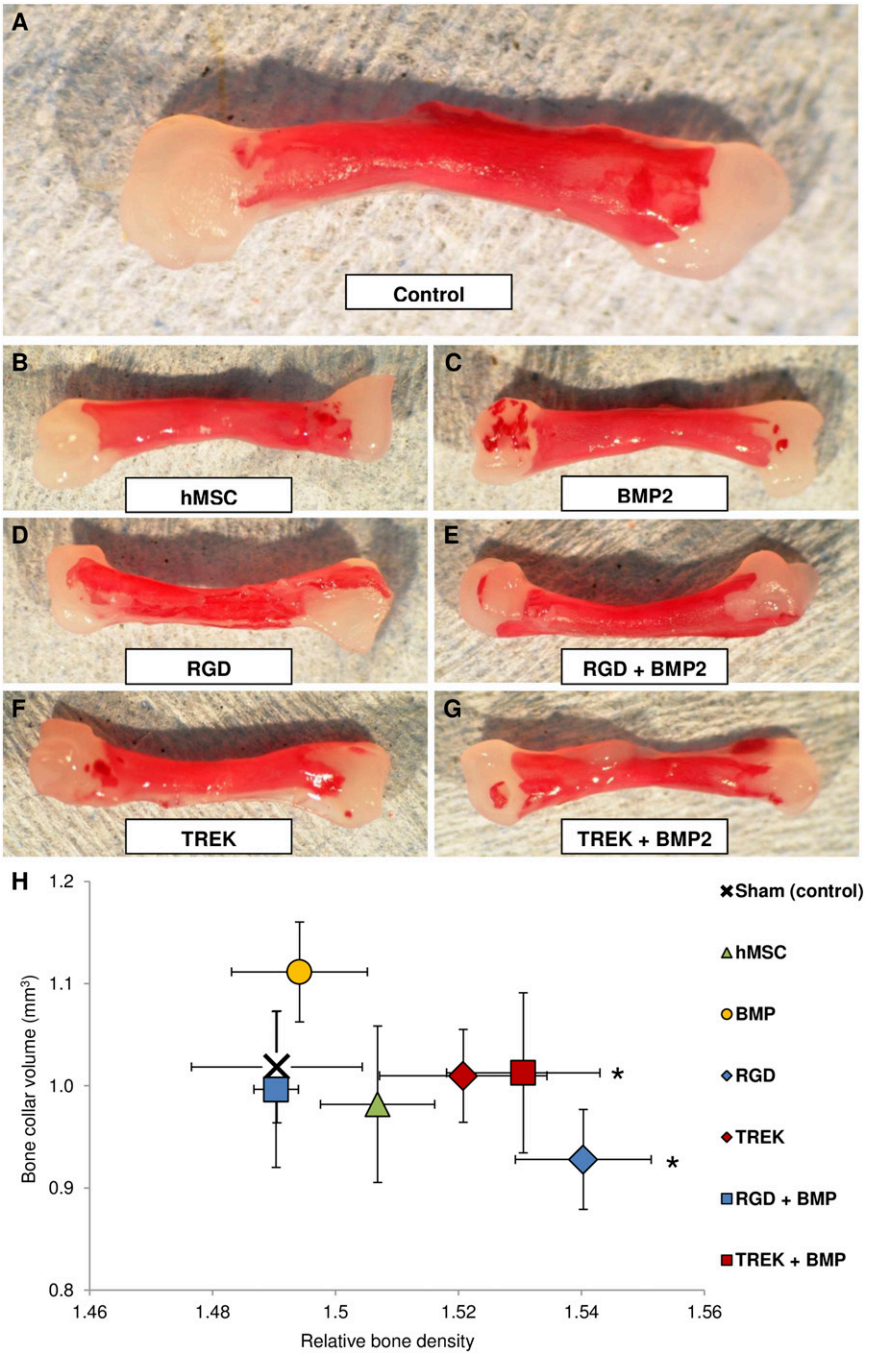

Figure 5. Mineralization in the chick fetal femur in response to nanoparticle-directed mechanotransduction and BMP2 release. **(A):** Calcium deposition (alizarin red S staining) of whole femurs after 2 weeks of in vitro organotypic culture shows that the bone collar is the only mineralization site in control (sham-injected) femurs. **(B, C):** When epiphyses were injected with hMSCs **(B)** or BMP2-releasing microparticles **(C)**, mineralization occurred at the injection sites. **(D, E):** Injection of cells prelabeled with either RGD-coated **(D)** or TREK-Ab-coated magnetic nanoparticles **(E)** showed increased bone formation, generally through extension of the bone collar into the epiphysis. **(F, G):** Combination injections of BMP2-releasing microparticles with RGD-labeled **(F)** or TREK-Ab-labeled **(G)** hMSCs showed both extension of the bone collar and areas of de novo mineralization at the injection site. **(H):** Quantification of the x-ray microtomography data reveals that injection of BMP2-releasing microparticles into the chick fetal femur caused an increase in the volume of bone formed (*y*-axis) compared with the sham-injected control but did not affect bone density (*x*-axis). Injections of unlabeled hMSCs caused a slight increase in the density of the bone (*x*-axis). Targeting TREK1 with magnetic nanoparticles and coinjecting BMP2-releasing microparticles resulted in a significant increase in bone density. Error bars show standard error of the mean ($n = 9$). $*, p < .05$. Abbreviations: BMP2, bone morphogenetic protein 2; hMSC, human mesenchymal stem cells; RGD, Arg-Gly-Asp tripeptide.

mechanisms have been described, including the integrin-cytoskeleton-nuclear matrix structure, stretch-activated cation channels within the cell membrane, G protein-dependent pathways and links between the cytoskeleton and the phospholipase C, and phospholipase A pathways [23, 24]. In practice, it is expected that most or all of these pathways are simultaneously excited to various extents, and the sensitivity of each semi-independent pathway is moderated by hormonal control

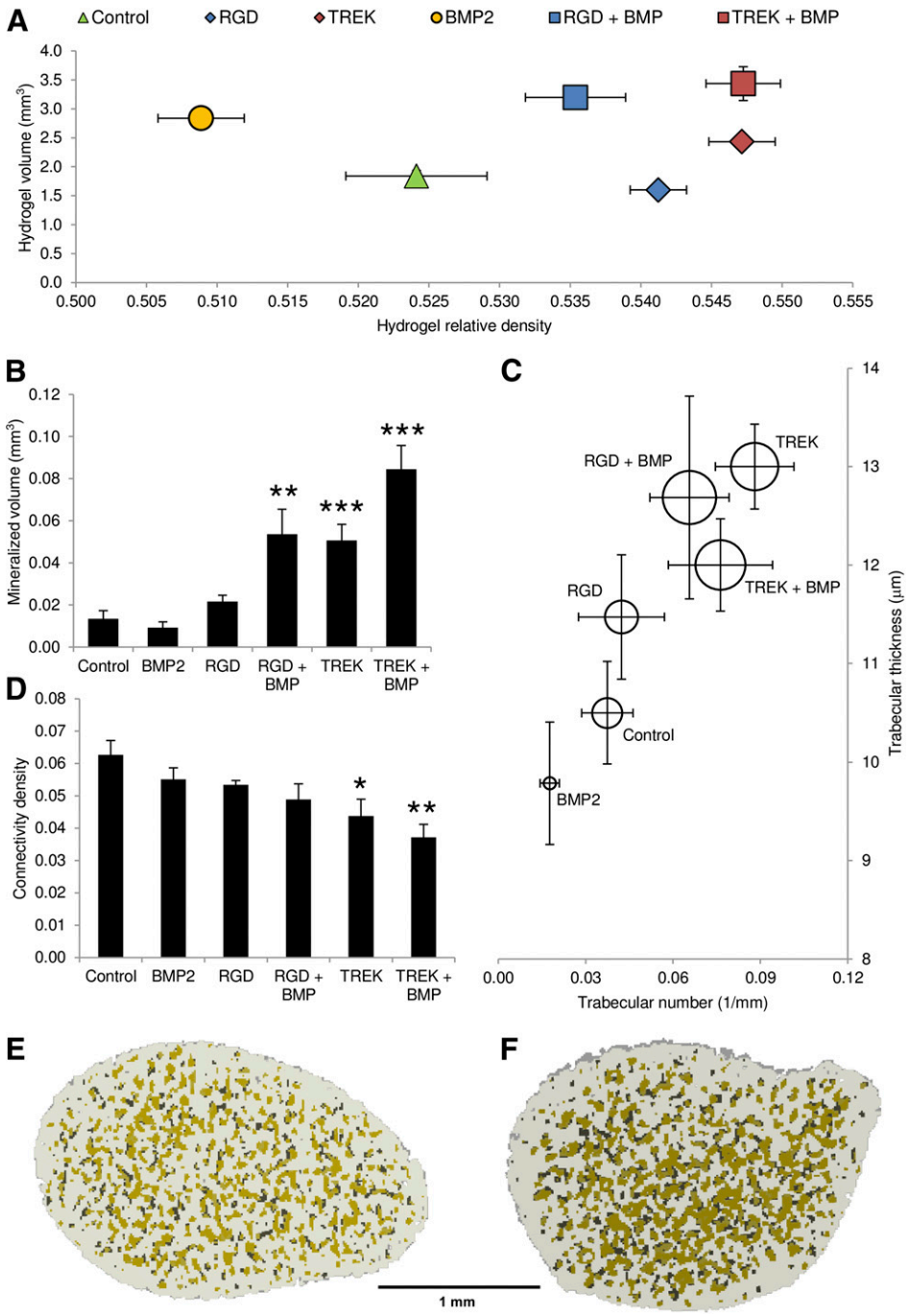

Figure 6. Combinations of magnetic nanoparticle-labeled human mesenchymal stem cells (hMSCs) and BMP2-releasing microparticles in 2.0% collagen hydrogels compared with either nanoparticles or BMP2 alone and controls, which were hMSCs alone. All hydrogels initially contracted within 72 hours of seeding; subsequent matrix formation and proliferation of MSCs resulted in an increase in hydrogel size by day 28 of the experiment. Significant differences were seen in the total size and density of the gels, which approximately match the positions of the equivalent groups from femur-injection studies (Fig. 4) as determined by x-ray microtomography data. **(A):** BMP2 alone resulted in an increase in hydrogel size, whereas prelabeling hMSCs with either magnetic nanoparticle caused an increase in gel density. Combinations of both BMP2-releasing microparticles and magnetic nanoparticles resulted in an increase in both volume and density, with the greatest effect seen from the combination of BMP2 and TREK-Ab labeled hMSCs. **(B):** Increasing the analysis threshold for the microtomography to quantify only the mineralized portion of the hydrogel revealed that the volume of the mineralizing high-density material was similar for the control and BMP2 alone, whereas cells treated with either nanoparticle in combination with BMP2 were significantly more mineralized. Nanoparticle-only and nanoparticle + BMP combinations resulted in the formation of more numerous and thicker mineralized regions within the hydrogel than either controls or BMP2 alone when analyzed as "trabeculae." **(C):** The diameter of each circle surrounding the data point reflects the average density of these regions. **(D–F):** These mineralized nodular regions were significantly less interconnected in the TREK-nanoparticle-containing groups compared with the control group **(D)** and are highlighted in green in the microtomography reconstructions, shown as cross-sections through the center of MSC-seeded hydrogels containing BMP2 particles alone **(E)**, compared with hydrogels containing BMP2 particles plus TREK-nanoparticle-labeled hMSC **(F)**. Error bars show standard error of the mean ($n = 7$). Scale bar = 1 mm. $*$, $p < .05$; $**$, $p < 0.01$; $***$, $p < .001$. Abbreviations: BMP2, bone morphogenetic protein 2; RGD, Arg-Gly-Asp tripeptide.

mechanisms, paracrine and autocrine signals from the reactive cell population, and changes in the transcriptome [23].

For skeletal remodeling, intense exercise and high levels of mechanical loading are generally presumed to be the most osteogenic stimuli, but evidence has shown that even brief exposure to high-frequency, low-intensity stimulation can provide a significant anabolic stimulus to bone and result in osteogenic differentiation of MSCs [25]. Controlled mechanotransduction in therapeutic MSCs may therefore present a novel, drug-free method suitable for inclusion in many translational regenerative strategies for bone repair.

In this investigation, functionalized magnetic nanoparticles were used to directly target and remotely activate mechanotransduction pathways via the integrin-cytoskeleton matrix (by targeting matrix-associated RGD-binding domains) or the stretch-activated ion channel TREK1. Previous research has generated evidence of direct force transduction by the nanoparticle-RGD-integrin complex and shown that the mechanically gated TREK1 ion channel can be remotely activated by attaching conjugated nanoparticles to the intracellular loop region and applying an oscillating magnetic field, resulting in observable changes in whole cell electrophysiology [11]. Directing mechanotransduction via either TREK1 or integrins has been reported to result in the osteogenic differentiation of mesenchymal stem cells [8–12] and their enhanced formation of extracellular matrix in an in vivo murine subcutaneous model [8]. In our in vitro (ex vivo) models, mechanotransduction via the TREK1 ion channel resulted in substantially greater mineralization than mechanotransduction via integrins, illustrating differences in sensory routes for mechanical stimuli in MSCs [26] and demonstrating the usefulness of conjugated magnetic nanoparticles as a customizable research tool for mechanobiology [7–9, 11, 12, 27].

In previously published work from this group, we successfully targeted TREK1 mechanotransduction to differentiate MSCs along an osteochondral lineage, resulting in the increased expression of both osteogenic genes (collagen I, osteopontin, and CBFA1) and chondrogenic genes (SOX9 and collagen II) [8]. Mineralization of the extracellular matrix in both the chick epiphysis and collagen scaffold was observed because of MSC differentiation in response to osteogenic medium, nanoparticle-based mechanotransduction, and BMP2 delivery. We hypothesize that paracrine signaling from stimulated, differentiating hMSCs may trigger osteogenic effects in the surrounding chick tissues, resulting in substantial bone mineralization from the relatively small number of injected therapeutic cells, and work is ongoing to investigate this. It was generally noted that untreated hMSCs alone did not greatly influence mineralization in either the chick femur or hydrogels, suggesting that a further stimulus such as mechanotransduction and/or delivered growth factors is required to induce downstream signaling, differentiation, and achievement of a fully active osteoblastic phenotype [2, 8, 21].

In the experiments reported here, we also noted that BMP2 generally resulted in an increase in bone formation, whereas mechanotransduction resulted in increases in bone density, further supporting the existing evidence that mechanotransduction acts as both a differentiation stimulus and amplifies the transduction of relevant growth factor signals from the surrounding environment [3]. Nanoparticle activation of TREK1 in particular was significant in increasing bone formation in both models, but most interestingly was found to act synergistically with the anabolic effects of BMP2, resulting in mineralized femurs and hydrogels with both increased volume and density, illustrating the importance of relevant mechanical stimuli acting in concert with growth factor signaling for optimum formation of a fully functional extracellular matrix [2, 3, 28, 29].

In all MSC-based strategies for tissue engineering, native endogenous growth factors in wound sites are crucial for orchestrating cell-mediated tissue regeneration [2, 3, 14, 15, 19]. As a deliverable growth factor, BMP2 is used in clinical applications in which substantial bone apposition is required, such as spinal fusion and treatment of nonunion [29]. In many current and proposed treatments, exogenous growth factor combinations are being used to coordinate, supplement, and amplify natural tissue regeneration [18–20]. Understanding the interactions between mechanotransduction pathways and growth factor signaling may therefore be key to determining and optimizing clinical effectiveness.

For example, it has recently been shown that mechanotransduction acts synergistically with BMP signaling in human fetal osteoblasts in vitro by increasing the intensity and duration of Smad phosphorylation early in the BMP signaling pathway, thereby reinforcing signal propagation [3]. In vivo, mechanical stimulation of a rat femur defect supplemented with BMP2 from a collagen sponge resulted in synergistic enhancement of bone repair: with the addition of BMP2, mechanically stimulated groups showed increased evidence of remodeling and reconstruction of the endosteal canal [29]. Similarly, the proteins involved in integrin-based mechanotransduction are seen to colocalize with BMP2 in certain models of distraction osteogenesis [30]. By directing mechanotransduction using magnetic nanoparticles, it is therefore possible to optimize the effective doses of exogenous growth factors by amplifying their intracellular cascades and potentially improving the clinical uses of therapeutic BMP treatments for various bone pathologies.

Magnetic nanoparticles are biocompatible and have existing regulatory approval as magnetic resonance imaging contrast agents (which potentially also permits in vivo monitoring of the cell therapy [31]) and offer several key advantages over other methods for translational mechanotransduction, chiefly that the injected cells can be specifically targeted, signaling pathways activated and precise forces applied without causing loading stresses to either the biomaterial scaffold or the bone-implant interface. Magnetic nanoparticles can also be used to apply dynamic loads to soft scaffolds that cannot be directly mechanically loaded, and the loading regimen can be controlled by altering the dose or size of the MNPs or by varying the external magnetic field strength. Single or multiple receptors can be chosen, and the nanoparticles can be functionalized with ligands or antibodies against either extracellular or intracellular targets, creating a versatile tool for clinical treatments and research [27].

Injectable therapies for regenerative medicine show great potential as a minimally invasive route for introducing therapeutic stem cells, drug delivery vehicles, and biomaterials efficiently to wound sites [32, 33]. Advances in biomaterials research, including thermosetting hydrogels that gelate at physiological temperatures, have revolutionized the opportunities for delivering cells, biomaterials, and growth factors [34]. This work demonstrates that providing the appropriate mechanical cues in conjunction with controlled release of growth factors to these injectable cell therapies can have a significant impact on improving osteogenesis and potentially improve tissue engineering approaches for translational medicine.

Conclusion

The synergistic promotion of osteogenesis by BMP2 delivery and nanoparticle-based mechanotransduction in models of endochondral ossification is an important conclusion that suggests substantial scope for improving cell-based orthopedic therapies. The work presented here suggests this technique has a potential contributory role in treating clinical bone defects, and in subsequent experiments, we aim to investigate mechanotransduction with combinations of other growth factors released from polymer microparticles. It is also possible that combinations of directed mechanotransduction with topographical and bioactive cues from surrounding tissues and orthopedic biomaterials may further enhance the osteogenic response, leading to fascinating directions for future collaborative research using these approaches. The combination of growth factor delivery and nanoparticle-directed mechanical stimulation presents an opportunity for optimized approaches for the rapid restoration of functional bone.

Acknowledgments

This work was supported by Biotechnology and Biological Sciences Research Council (BBSRC) Grants BB/G010560/1 (to Keele University) and BB/G010617/1 (to Nottingham University). We thank the BBSRC for supporting this work through a strategic longer and larger grant, Grant BB/G010560/1. We also thank our collaborators in groups led by Prof. Richard Oreffo (University of Southampton) and Prof. Molly Stevens (Imperial College London). In particular, we thank Dr. Lisa White, Dr. Helen Cox, and Dr. Omar Qutachi (University of Nottingham) for their work on developing the BMP2-releasing microparticles technology used in this investigation.

Author Contributions

J.R.H.: conception and design, collection and/or assembly of data, data analysis and interpretation, manuscript writing, final approval of manuscript; M.R.: provision of study material or patients, collection and/or assembly of data, data analysis and interpretation, manuscript writing, final approval of manuscript; H.R.: provision of study material or patients, manuscript writing, final approval of manuscript; K.M.S.: provision of study material or patients, final approval of manuscript; A.J.E.H.: conception and design, financial support, administrative support, final approval of manuscript.

Disclosure of Potential Conflicts of Interest

A.J.E.H. has uncompensated employment, intellectual property rights, research funding, and stock options.

References

1 Simon JA, Ricci JL, Di Cesare PE. Bioresorbable fracture fixation in orthopedics: A comprehensive review. Part I. Basic science and preclinical studies. Am J Orthop 1997;26:665–671.

2 Kim IS, Song YM, Cho TH et al. Synergistic action of static stretching and BMP-2 stimulation in the osteoblast differentiation of C2C12 myoblasts. J Biomech 2009;42:2721–2727.

3 Kopf J, Petersen A, Duda GN et al. BMP2 and mechanical loading cooperatively regulate immediate early signalling events in the BMP pathway. BMC Biol 2012;10:37.

4 Griffin XL, Costello I, Costa ML. The role of low intensity pulsed ultrasound therapy in the management of acute fractures: A systematic review. J Trauma 2008;65:1446–1452.

5 Frias C, Reis J, Capela e Silva F et al. Polymeric piezoelectric actuator substrate for osteoblast mechanical stimulation. J Biomech 2010; 43:1061–1066.

6 Walker NA, Denegar CR, Preische J. Low-intensity pulsed ultrasound and pulsed electromagnetic field in the treatment of tibial fractures: A systematic review. J Athl Train 2007;42:530–535.

7 Wimpenny I, Markides H, El Haj AJ. Orthopaedic applications of nanoparticle-based stem cell therapies. Stem Cell Res Ther 2012;3:13.

8 Kanczler JM, Sura HS, Magnay J et al. Controlled differentiation of human bone marrow stromal cells using magnetic nanoparticle technology. Tissue Eng Part A 2010;16:3241–3250.

9 Hughes S, Dobson J, El Haj AJ. Magnetic targeting of mechanosensors in bone cells for tissue engineering applications. J Biomech 2007; 40(suppl 1):S96–S104.

10 Hughes S, Magnay J, Foreman M et al. Expression of the mechanosensitive 2PK+ channel TREK-1 in human osteoblasts. J Cell Physiol 2006;206:738–748.

11 Hughes S, McBain S, Dobson J et al. Selective activation of mechanosensitive ion channels using magnetic particles. J R Soc Interface 2008;5: 855–863.

12 Cartmell SH, Dobson J, Verschueren SB et al. Development of magnetic particle techniques for long-term culture of bone cells with intermittent mechanical activation. IEEE Trans Nanobioscience 2002;1:92–97.

13 Henstock JR, Rotherham M, Rose JB et al. Cyclic hydrostatic pressure stimulates enhanced bone development in the foetal chick femur in vitro. Bone 2013;53:468–477.

14 Kanczler JM, Smith EL, Roberts CA et al. A novel approach for studying the temporal modulation of embryonic skeletal development using organotypic bone cultures and microcomputed tomography. Tissue Eng Part C Methods 2012;18:747–760.

15 Smith EL, Kanczler JM, Roberts CA et al. Developmental cues for bone formation from parathyroid hormone and parathyroid hormone-related protein in an ex vivo organotypic culture system of embryonic chick femora. Tissue Eng Part C Methods 2012;18:984–994.

16 Hamburger V, Hamilton HL. A series of normal stages in the development of the chick embryo. J Morphol 1951;88:49–92.

17 Barbetta A, Bedini R, Pecci R et al. Role of x-ray microtomography in tissue engineering. Ann Ist Super Sanita 2012;48:10–18.

18 Kirby GTS, White LJ, Rahman CV et al. PLGA-based microparticles for the sustained release of BMP-2. Polymers 2011;3:571–586.

19 Saif J, Schwarz TM, Chau DY et al. Combination of injectable multiple growth factor-releasing scaffolds and cell therapy as an advanced modality to enhance tissue neovascularization. Arterioscler Thromb Vasc Biol 2010; 30:1897–1904.

20 Kanczler JM, Ginty PJ, White L et al. The effect of the delivery of vascular endothelial growth factor and bone morphogenic protein-2 to osteoprogenitor cell populations on bone formation. Biomaterials 2010;31: 1242–1250.

21 Nowlan NC, Sharpe J, Roddy KA et al. Mechanobiology of embryonic skeletal development: Insights from animal models. Birth Defects Res C Embryo Today 2010;90:203–213.

22 Mullender M, El Haj AJ, Yang Y et al. Mechanotransduction of bone cells in vitro: Mechanobiology of bone tissue. Med Biol Eng Comput 2004;42:14–21.

23 Duncan RL, Turner CH. Mechanotransduction and the functional response of bone to mechanical strain. Calcif Tissue Int 1995;57: 344–358.

24 Kearney EM, Farrell E, Prendergast PJ et al. Tensile strain as a regulator of mesenchymal stem cell osteogenesis. Ann Biomed Eng 2010;38:1767–1779.

25 Ozcivici E, Luu YK, Adler B et al. Mechanical signals as anabolic agents in bone. Nat Rev Rheumatol 2010;6:50–59.

26 Hamill OP, Martinac B. Molecular basis of mechanotransduction in living cells. Physiol Rev 2001;81:685–740.

27 MacQueen L, Sun Y, Simmons CA. Mesenchymal stem cell mechanobiology and emerging experimental platforms. J R Soc Interface 2013;10:20130179.

28 McKay WF, Peckham SM, Badura JM. A comprehensive clinical review of recombinant human bone morphogenetic protein-2 (INFUSE Bone Graft). Int Orthop 2007;31:729–734.

29 Schwarz C, Wulsten D, Ellinghaus A et al. Mechanical load modulates the stimulatory

effect of BMP2 in a rat nonunion model. Tissue Eng Part A 2013;19:247–254.

30 Rhee ST, Buchman SR. Colocalization of c-Src (pp60src) and bone morphogenetic protein 2/4 expression during mandibular distraction osteogenesis: In vivo evidence of their role within an integrin-mediated mechanotransduction pathway. Ann Plast Surg 2005;55:207–215.

31 Markides H, Kehoe O, Morris RH et al. Whole body tracking of superparamagnetic iron oxide nanoparticle-labelled cells: A rheumatoid arthritis mouse model. Stem Cell Res Ther 2013; 4:126.

32 Gong C, Qi T, Wei X et al. Thermosensitive polymeric hydrogels as drug delivery systems. Curr Med Chem 2013;20:79–94.

33 Johnson TD, Christman KL. Injectable hydrogel therapies and their delivery strategies for treating myocardial infarction. Expert Opin Drug Deliv 2013;10:59–72.

34 Lin Z, Cao S, Chen X et al. Thermoresponsive hydrogels from phosphorylated ABA triblock copolymers: A potential scaffold for bone tissue engineering. Biomacromolecules 2013;14:2206–2214.